

Design and Analysis of Optimal Threshold Offloading Algorithm for LTE Femtocell/Macrocell Networks

Wei-Han Chen, Yi Ren, Chia-Wei Chang, and Jyh-Cheng Chen, *Fellow, IEEE*

Abstract

LTE femtocells have been commonly deployed by network operators to increase network capacity and offload mobile data traffic from macrocells. A User Equipment (UE) camped on femtocells has the benefits of higher transmission rate and longer battery life due to its proximity to the base stations. However, various user mobility behaviors may incur network signaling overhead and degrade femto-cell offloading capability. To efficiently offload mobile data traffic, we propose an optimal Threshold Offloading (TO) algorithm considering the trade-off between network signaling overhead and femtocell offloading capability. In this paper, we develop an analytical model to quantify the trade-off and validate the analysis through extensive simulations. The results show that the TO algorithm can significantly reduce signaling overhead at minor cost of femtocell offloading capability. Moreover, this work offers network operators guidelines to set optimal offloading threshold in accordance with their management policies in a systematical way.

Keywords

LTE, Offloading, Femtocell, Performance Analysis

I. INTRODUCTION

The Long Term Evolution-Advanced (LTE-A) [1] standardized by the 3rd Generation Partnership Project (3GPP) provides high speed wireless data transmission services: up to 100 Mbit/s peak data rates for high mobility access and 1 Gbit/s for low mobility users. LTE-A together with

The authors are with the Department of Computer Science, National Chiao Tung University, Hsinchu 300, Taiwan (E-mail: {whchen, yiren, chwchang, jcc}@cs.nctu.edu.tw)

ubiquitous Internet access offered by various mobile devices leads to explosive growth of mobile data traffic in the past few years. According to the 2014 annual report from AT&T, mobile data traffic on their network increased 100,000% from 2007 to 2014 [2]. A Cisco report states global mobile data traffic has reached 2.5 exabytes per month at the end of 2014. It also forecasts that mobile data traffic will increase almost tenfold between 2014 and 2019 [3]. The unprecedented data traffic growth pushes mobile networks to their operational limits and motivates network operators to seek for efficient solutions that can help relieve network congestion.

Data offloading is one of such solutions that alleviate network congestion by moving mobile data traffic from a congested Radio Access Network (RAN) to a capacious target RAN. Generally, data offloading can be classified into two categories: (1) homogeneous network data offloading, and (2) heterogeneous network data offloading. The former offloads mobile data traffic of a User Equipment (UE) within 3GPP RANs, e.g., from a macrocell to a femtocell. In LTE-A network, a macrocell refers to the radio coverage of an evolved NodeB (eNB), and a femtocell (also called a small cell) refers to that of a Home evolved NodeB (HeNB). Fig. 1 illustrates the general LTE-A architecture. On the other hand, the latter one offloads the mobile data traffic from a 3GPP RAN to a non-3GPP RAN, e.g., from a macrocell to a Wi-Fi network.

In this paper, we focus on data offloading in homogeneous networks. The emergent femtocell extends the coverage of cellular networks and makes data offloading in homogeneous networks a promising solution. From network operators' point of view, femtocells can extend network coverage, offload mobile data traffic from macrocells, and increase network capacity [4]. From users' point of view, femtocells enable higher transmission rate and longer battery life since UEs receive better signal strength and consume less energy [5]. With all these attractive benefits, femtocells are commonly accepted by network operators as an effective offloading technique and massively deployed in urban and metropolitan areas. According to [6] reported in 2014, Korea Telecom (KT) has deployed more than 10,000 small cells in the Seoul metropolitan area and a further 8,000 in greater Seoul, which houses over half population in South Korea.

However, many researchers have pointed out that femtocell offloading may not always guarantee aforementioned benefits and may cause network signaling overhead due to various user mobility behaviors [7]–[14]. For instance, if high mobility users reside in a femtocell for a short period of time, only small amount of data can be offloaded. However, they trigger two handover procedures and incur signaling overhead in the core network when they move into and out of a

femtocell. For simplicity, we call this behavior as *transient handover*. The transient handovers not only degrade Quality of Experience (QoE) of mobile users but also reduce the availability of femtocells for legitimate users, i.e., reduce system capacity. Thus, in order to tackle the transient handover issue and offload mobile data traffic from macrocells in a cost-effective way, it is important to address *when* and *how* should a UE handover into a femtocell when the UE approaches the boundary of the femtocell. It is essentially a trade-off between network signaling overhead and femtocell offloading capability.

In this paper, we propose an optimal algorithm to offload mobile data traffic to femtocells and provide a mathematical model to quantify its performance. Our analytical model and simulation results show consistent findings that the proposed algorithm significantly reduces signaling overhead and sacrifices little femtocell offloading capability. The contributions of this paper are twofold:

- First, we propose an effective algorithm for femtocell traffic offloading considering the trade-off between network signaling overhead and femtocell offloading capability. Moreover, the proposed algorithm is simple. Thus, it is easy to implement.
- Second, we provide an analytical model to investigate the performance of our proposed algorithm, which is further validated through extensive simulations. In addition, our mathematical analysis offers guidelines for network operators on setting optimal offloading threshold in a systematic way.

The remaining parts of the paper are organized as follows. Section II introduces the background. Section III presents the related work. Section IV describes the proposed Threshold Offloading (TO) algorithm. The analytical model is presented in Section V. The simulation and numerical results are given in Section VI. Section VII presents the optimal TO algorithm. Section VIII summarizes the paper.

II. BACKGROUND

Fig. 1 shows an exemplary scenario that a UE has an active session while passing through the coverage areas of an eNB and a set of HeNBs, typically with radius within 2,000 meters and 20 meters, respectively [4]. The UE connects to the core network via either the eNB or one of the HeNBs. In the core network, a Mobility Management Entity (MME) handles bearer management, mobility management, and control plane signaling. A Serving Gateway (S-GW)

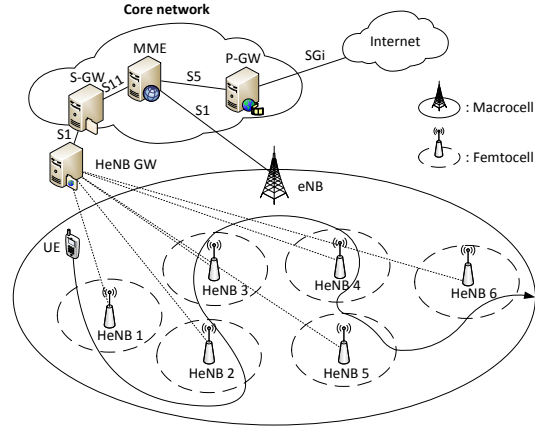


Fig. 1: The general LTE-A architecture and an exemplary handover scenario.

forwards user packets between the UE and the core network. The routing between the core network and the Internet is responsible by a Packet Data Network Gateway (P-GW). Details of the core network, MME, S-GW and P-GW can be found in [1].

Fig. 2 shows the handover procedure specified in the 3GPP standard [1], referred to as the baseline handover procedure in this paper. In the figure, solid lines indicate signaling messages, and dashed lines represent user data traffic. There are three phases in the baseline procedure: handover preparation, handover execution, and handover completion. Since the proposed algorithm only involves in handover preparation phase, we elaborate the handover preparation phase as follows:

- Step 1: The serving eNB informs the UE in which event the received signal strength should be reported through a configuration message, and the UE keeps track of the received signal strength of its serving cell and neighboring cells.
- Step 2: Upon a specified event¹ happens, the UE sends measurement reports to the eNB.
- Step 3: The serving eNB decides whether to initiate a handover (HO) procedure to the selected target cell based on the information received from the UE measurement reports and the status of the neighboring cells.
- Step 4: The serving eNB sends a handover request as well as the UE context (e.g., security

¹There are several measurement report triggering events defined in the 3GPP standard: event A1-A6, B1, B2, C1, and C2. For example, event A3 is triggered when signal level from neighbor cell becomes amount-of-offset better than serving cell. Further details can be found in [15].

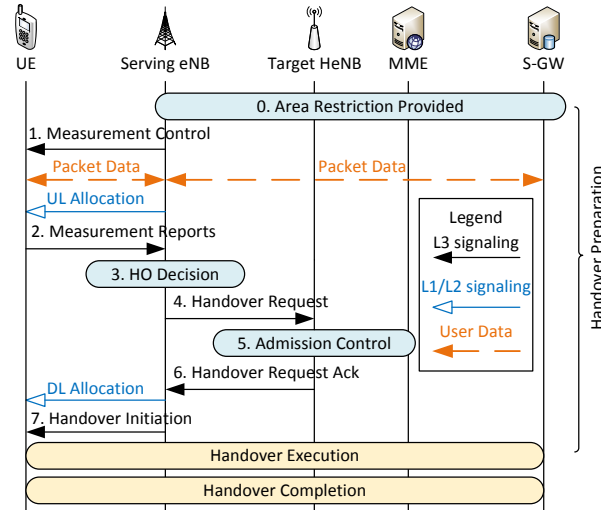


Fig. 2: Handover procedure specified in the 3GPP standard.

and QoS context) to the target HeNB.

- Step 5: The admission control ensures that the UE will be served with enough bandwidth and guarantees the UE's QoS requirements. In addition, it checks whether a UE is legitimate to access its resources.
- Step 6: If the target HeNB is capable of providing the requested service quality, it informs the serving eNB with a Handover Request Ack.
- Step 7: The serving eNB sends a control message to the UE to initiate the handover procedure.

For further understanding of the handover procedure, readers can refer to [1] for details.

III. RELATED WORK

Many studies [7]–[14] have been proposed for homogeneous network data offloading. The authors in [7] first identified the frequent and unnecessary handover problem for hierarchical network environment. They proposed a Call Admission Control (CAC) mechanism at target HeNB, which significantly reduces the impacts of transient handovers. However, the work did not provide analysis and guidelines for operators on how to set optimal values for the essential parameters. The authors in [8] later extended the problem to hybrid access mode HeNBs and classified users into two groups: pre-registered and unregistered. Unregistered users are not

allowed to handover into femtocells so a portion of frequent handovers are efficiently avoided. However, the frequent handover problem still exists for pre-registered users.

In [10]–[12], the authors considered Received Signal Strength (RSS) and UE’s moving speed to reduce unnecessary handover executions. The authors in [10] designed two novel handover algorithms based on RSS and velocity information from UEs: Velocity and Signal Handover (VSHO) and Unequal Handover (UHO). In VSHO, a UE will handover into a femtocell if its velocity is within the maximum handover velocity level and its RSS level is above the minimum RSS level. As an improvement of VSHO, UHO further considers the difference of signal levels between the eNB and the HeNB. The authors in [12] took UE mobility state and application type into consideration, where UE mobility behaviors are classified into three states: low (0-15 km/h), medium (15-30 km/h), and high (above 30 km/h). Transient handovers caused by high mobility UEs are avoided effectively. In [11], in addition to UE mobility state and application type, the authors further used proactive handover procedure to reduce packet loss for real-time services. However, in LTE networks, velocity measurement of a UE causes extra costs and may not be accurately obtained.

Recent works [9], [13], [14] further considered UE’s signal information. In [13], the authors proposed Double Threshold Algorithm (DTA) which uses two thresholds of Signal to Interference and Noise Ratio (SINR) to determine whether a handover procedure should be performed. Because DTA heavily depends on accurate measurement of SINR, serious interference in densely-deployed metropolitan areas will cause inaccurate measurements and makes it ineffective in those areas. In [9], the authors proposed a novel Reducing Handover Cost (RHC) mechanism in that femtocell-to-macrocell handover requests are delayed for a period of time when UEs move out of a femtocell. The work reduces signaling cost caused by transient handovers. However, RHC may not have the desired outcome if the HeNBs are not in close proximity to each other. Our recent work [14] proposes a threshold offloading algorithm considering the trade-off between network signaling overhead and femtocell offloading capability. The algorithm significantly reduces signaling overhead at minor cost of femtocell offloading capability. However, the work did not consider how to select an optimal threshold value for the trade-off.

There are many studies on heterogeneous network data offloading, but we only list some representative ones since our focus is on homogeneous network data offloading. A system called Wiffler proposed in [16] exploits the delay tolerance of content and the contacts with fixed Access

Points (APs). Wiffler predicts future encounters with APs and defers data transmission only if the transfer can be finished within the application's tolerable threshold and reduce cellular data usage. The work [17] proposes to use cognitive radio techniques to offload mobile traffic to wireless APs, where the trade-off between optimal mobile traffic offloading and energy consumption was studied. The scheme is proved to work well and can save at least 50% energy of base stations. The authors in [18] conducted quantitative studies on the benefit of Wi-Fi offloading with respect to network operators and mobile users. They collected trace data for two and a half weeks from Seoul, Korea, and analyzed Wi-Fi availability. The results reveal that non-delayed Wi-Fi offloading could already relieve a large portion of cellular data traffic, and confirm that delayed Wi-Fi offloading has even more promising potential.

IV. PROPOSED THRESHOLD OFFLOADING (TO)

The transient handover consists of two parts: macrocell-to-femtocell and femtocell-to-macrocell handover. The proposed Threshold Offloading (TO) is employed at the serving eNB to prevent undesired macrocell-to-femtocell transient handovers, and so the following femtocell-to-macrocell handovers are also prevented.

The proposed TO requires only minor modification of the 3GPP standard, shown in Fig. 3. When a UE enters a femtocell and meets the handover triggering requirements, the macrocell-to-femtocell handover request is deferred at the serving eNB until a predefined offloading threshold t_o is reached. If the UE leaves the femtocell before t_o expires, no handover is triggered. Otherwise, the handover request will be sent to the target HeNB if t_o has expired and the triggering condition for handover still exists. Fig. 3 illustrates the flow chart for the TO.

The parameter, t_o , determines the efficiency of the proposed TO. For instance, more signaling overhead can be reduced by setting a larger t_o , but it will degrade femtocell offloading capability because less time UEs will be offloaded to femtocells. Although the proposed TO sounds intuitive, how to set t_o properly is nontrivial. In next section, we present a mathematical model to determine t_o in a systematic way.

Note that, in the handover process, t_o should be distinguished from the parameter, time-to-trigger (TTT) value, which is mainly for preventing ping-pong effect and radio link failure. Our proposed TO does not use the TTT value to delay handover so that eNBs are able to acquire information of UEs' radio connection in a timely manner. Therefore, radio link failures due to

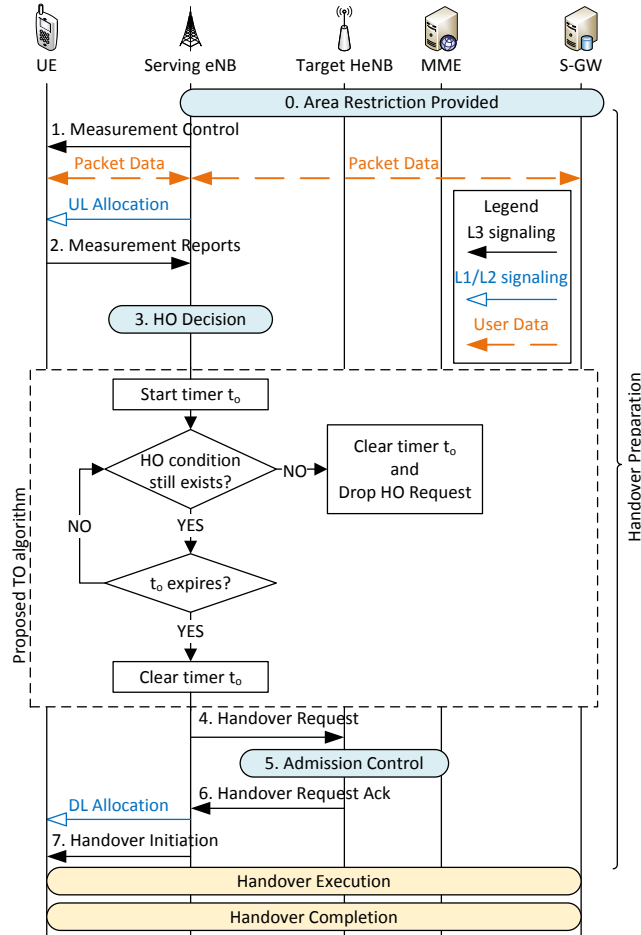


Fig. 3: The proposed TO algorithm.

the delayed handover process are avoided.

V. ANALYTICAL MODEL

In this section, we investigate the trade-off between *signaling overhead* and femtocell *offloading capability*. We first propose a mathematical model to quantify the characteristics of the trade-off. Next, the impacts of the offloading threshold t_o are studied by two performance metrics: *signaling overhead reduction ratio* $\Theta(t_o)$ and *offloading capability loss ratio* $\Lambda(t_o)$.

We define signaling overhead reduction ratio $\Theta(t_o)$ ($0 < \Theta(t_o) \leq 1$) as:

$$\Theta(t_o) = \frac{E[N_b] - E[N_t(t_o)]}{E[N_b]}, \quad (1)$$

where $N_t(t_o)$ and N_b are the total number of handovers during a session with and without

TO, respectively. $\Theta(t_o)$ indicates at what percentage the proposed TO reduces total number of handovers in a session. The higher $\Theta(t_o)$ is, the better the TO performs. Next, we define offloading capability loss ratio $\Lambda(t_o)$ ($0 < \Lambda(t_o) \leq 1$) as:

$$\Lambda(t_o) = \frac{E[T_t(t_o)]}{E[T_b]}, \quad (2)$$

where $T_t(t_o)$ and T_b are the total time that the session is served in femtocell with and without TO, respectively. No assumptions made on traffic types or traffic distributions, we use time ratio to represent the possibility that a UE's session can be served by femtocells. Since the TO will reduce the amount of time offloaded to femtocell during a session, $\Lambda(t_o)$ indicates how much offloading capability the TO can remain compared to the baseline scheme in 3GPP standard.

There is an inverse relationship between the two performance metrics, so our design goal is to find an optimal t_o such that it can bring $\Theta(t_o)$ and $\Lambda(t_o)$ to their possible maxima.

The radio coverage areas of femtocells overlapped with a macrocell may be continuous or discontinuous. The difference between them is that, in discontinuous case, a UE can be at most under one femtocell coverage, therefore there is only one target HeNB to handover. While in continuous case, a UE can be under multiple femtocell coverage, and there are multiple target HeNBs, which complicates UEs' measurement reporting and handover decision. In this study, we first consider the discontinuous case and leave the continuous one as our future work.

Because the cell shape (e.g. hexagonal or circular), the cell size, UE moving speed, and their moving direction are hard to be characterized, in this paper, the mobility behavior of a UE is modeled by the length of Cell Residence Time (CRT). This is commonly adopted in previous studies [9], [19]. In our analytical model, when a UE travels in the macrocell, it alternately stays in the macrocell and the femtocells. A UE's session can be categorized into four cases, as shown in Fig. 4. In Fig. 4a, a UE's session starts and ends in a macrocell. In Fig. 4b, a UE's session starts in a macrocell but ends in a femtocell. Fig. 4c shows that a UE's session starts in a femtocell and ends in a macrocell. A UE's session starts and ends in a femtocell is depicted in Fig. 4d.

During a UE's session, for $i \geq 1$, the i^{th} CRT in a macrocell is denoted by t_{m_i} and the i^{th} CRT in a femtocell is denoted by t_{f_i} . For $i = 0$, t_{m_0} refers to previous macrocell residence time in which a session starts, and the same for t_{f_0} . Next, we list the assumptions in our analysis:

- 1) Both macrocell and femtocell CRT, t_{m_i} and t_{f_i} , are i.i.d. and generally distributed as $f_m(t)$ and $f_f(t)$, with mean $1/\eta_m$ and $1/\eta_f$, respectively. Their Laplace transforms are denoted as $f_m^*(s)$ and $f_f^*(s)$.
- 2) The session length, t_s , follows exponential distribution with mean $1/\eta_s$, and with the probability density function (pdf) $f_s(t) = \eta_s e^{-\eta_s t}$.
- 3) The offloading threshold, t_o , is exponentially distributed with mean $1/\eta_o$, and with the pdf $f_o(t) = \eta_o e^{-\eta_o t}$.

During a session, we define t_{s_i} as the period of time from a UE's i^{th} handover into a femtocell to the time the session ends. Since t_s is exponentially distributed, from the memoryless property of exponential process [20], t_{s_i} has the same distribution as t_s , i.e., its pdf $f_{s_i}(t) = \eta_s e^{-\eta_s t}$. We summarize the notations used in our analytical model in Table I.

A. Derivation of Signaling Overhead Reduction Ratio $\Theta(t_o)$

Recall that $\Theta(t_o) = (E[N_b] - E[N_t(t_o)]) / E[N_b]$. In the following, we derive $E[N_b]$ and $E[N_t(t_o)]$, respectively. There are four possible scenarios for a UE session, as shown in Fig. 4. We classify them into two cases: Case 1 for the session starting in a macrocell, as shown in Figs. 4a and 4b, and Case 2 for the session starting in a femtocell, as shown in Figs. 4c and 4d. The UE stays in femtocell and macrocell alternatively as it moves during a session. From the alternative renewal process [20], we can obtain:

$$Pr[\text{Case1}] = \frac{E[t_{m_i}]}{E[t_{m_i}] + E[t_{f_i}]} = \frac{\eta_f}{\eta_f + \eta_m}, \quad (3)$$

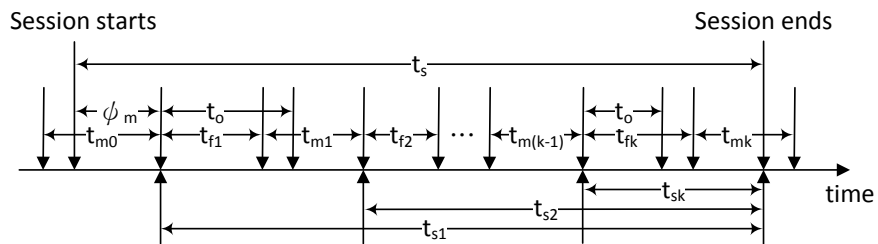
$$Pr[\text{Case2}] = \frac{E[t_{f_i}]}{E[t_{m_i}] + E[t_{f_i}]} = \frac{\eta_m}{\eta_f + \eta_m}. \quad (4)$$

Following the mathematical results of [21], we directly have:

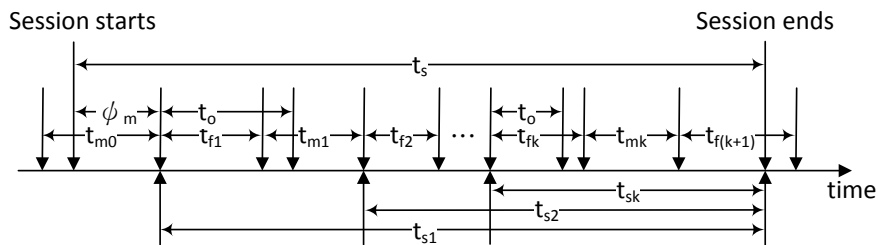
$$E[N_b] = \sum_{k=1}^{\infty} k Pr[N_b = k] = \frac{2\eta_m\eta_f}{\eta_s(\eta_m + \eta_f)}, \quad (5)$$

$$\alpha = Pr[t_o < t_{f_i} | t_{f_i} < t_{s_i}] = \frac{f_f^*(\eta_s) - f_f^*(\eta_s + \eta_o)}{f_f^*(\eta_s)}, \quad (6)$$

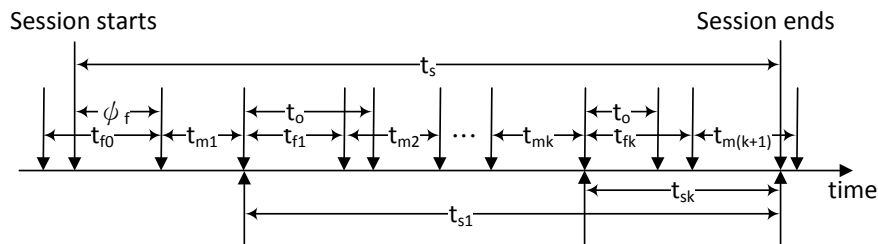
$$\beta = Pr[t_o < t_{s_i} | t_{s_i} < t_{f_i}] = \frac{\left(\frac{\eta_o}{\eta_s + \eta_o}\right) + \left(\frac{\eta_s}{\eta_s + \eta_o}\right) f_f^*(\eta_s + \eta_o) - f_f^*(\eta_s)}{1 - f_f^*(\eta_s)}, \quad (7)$$



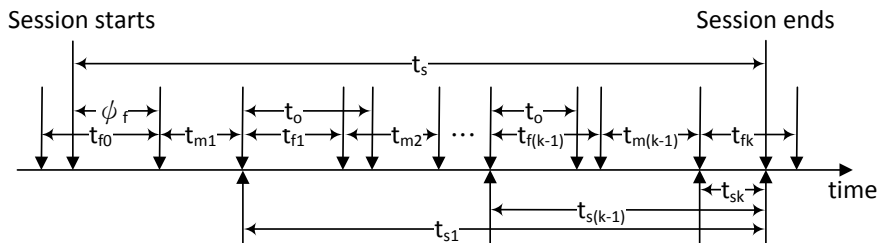
(a) Case 1-1: A UE session starts and ends in a macrocell.



(b) Case 1-2: A UE session starts in a macrocell and ends in a femtocell.



(c) Case 2-1: A UE session starts in a femtocell and ends in a macrocell.



(d) Case 2-2: A UE session starts and ends in a femtocell.

Fig. 4: The timing diagram for the four handover scenarios of a UE session

where α and β are the conditional probability that a UE handovers into a femtocell during t_{f_i} , given that the session does not end during this t_{f_i} and ends during this t_{f_i} , respectively. Then, to derive $E[N_t(t_o)]$, we express it as:

TABLE I: List of Parameters

	Parameter
Session length	t_s
Femtocell residence time	t_f
Macrocell residence time	t_m
Offloading threshold	t_o
Offloading time during the session with TO	T_t
Offloading time during the session without TO	T_b
Total number of handovers during the session with TO	N_t
Total number of handovers during the session without TO	N_b
Number of macrocell-to-femtocell crossings during the session	N_f
Number of femtocell-to-macrocell crossings during the session	N_m
Number of macrocell-to-femtocell handovers during the session	N_h
Residual life of macrocell residence time	ψ_m
Residual life of femtocell residence time	ψ_f
Probability density function of t_s	$f_s(t)$
Probability density function of t_f	$f_f(t)$
Probability density function of t_m	$f_m(t)$
Probability density function of t_o	$f_o(t)$
Mean session length	$1/\eta_s$
Mean femtocell residence time	$1/\eta_f$
Mean macrocell residence time	$1/\eta_m$
Mean offloading threshold	$1/\eta_o$

$$\begin{aligned}
& E[N_t(t_o)] \\
& = Pr[\text{Case1}]E[N_t(t_o)|\text{Case1}] + Pr[\text{Case2}]E[N_t(t_o)|\text{Case2}] .
\end{aligned} \tag{8}$$

Let N_f and N_m be the total number of macrocell-to-femtocell crossings during t_s and the

total number of femtocell-to-macrocell crossings during t_s , respectively, where $N_f + N_m = N_b$.

Case 1-1: The number of cell crossings is even, i.e., $N_{1,b} = 2i, \forall i \in \mathbb{N}_{>0}$, and $N_f = N_m = \frac{N_{1,b}}{2}$. For Case 1-1, thus, we have:

$$\begin{aligned}
& E[N_t(t_o)|\text{Case1-1}] \\
&= \sum_{i=1}^{\infty} \sum_{k=0}^i (i+k) Pr[N_t(t_o) = i+k | N_{1,b} = 2i] Pr[N_{1,b} = 2i] \\
&= \sum_{i=1}^{\infty} \sum_{k=0}^i [(i+k) \binom{i}{k} \alpha^k (1-\alpha)^{i-k}] Pr[N_{1,b} = 2i] \\
&= \sum_{i=1}^{\infty} [(1+\alpha)i] \left(\frac{\eta_m}{\eta_s}\right) f_f^*(\eta_s) [1 - f_m^*(\eta_s)]^2 [f_m^*(\eta_s) f_f^*(\eta_s)]^{i-1} \\
&= \frac{\eta_m f_f^*(\eta_s) [1 - f_m^*(\eta_s)]^2 (1+\alpha)}{\eta_s (1 - f_m^*(\eta_s) f_f^*(\eta_s))^2}. \tag{9}
\end{aligned}$$

Case 1-2: The number of cell crossings is odd, i.e., $N_{1,b} = 2i + 1, \forall i \in \mathbb{N}$, $N_f = \frac{N_{1,b}+1}{2}$ and $N_m = \frac{N_{1,b}-1}{2}$. For Case 1-2, thus, we have:

$$\begin{aligned}
& E[N_t(t_o)|\text{Case1-2}] \\
&= \sum_{i=0}^{\infty} \left[\beta + \sum_{k=0}^i (i+k) Pr[N_t(t_o) = i+k | N_{1,b} = 2i+1] \right] \\
&\quad \times Pr[N_{1,b} = 2i+1] \\
&= \sum_{i=0}^{\infty} \left(\beta + \sum_{k=0}^i (i+k) \binom{i}{k} \alpha^k (1-\alpha)^{i-k} \right) Pr[N_{1,b} = 2i+1] \\
&= \sum_{i=0}^{\infty} [(1+\alpha)i + \beta] \left(\frac{\eta_m}{\eta_s}\right) [1 - f_f^*(\eta_s)] [1 - f_m^*(\eta_s)] [f_m^*(\eta_s) f_f^*(\eta_s)]^i \\
&= \frac{\eta_m [1 - f_f^*(\eta_s)] [1 - f_m^*(\eta_s)] [\beta + (1+\alpha - \beta) f_m^*(\eta_s) f_f^*(\eta_s)]}{\eta_s (1 - f_m^*(\eta_s) f_f^*(\eta_s))^2}. \tag{10}
\end{aligned}$$

Case 2-1: The number of cell crossings is odd, i.e., $N_{2,b} = 2i + 1, \forall i \in \mathbb{N}$, $N_f = \frac{N_{2,b}-1}{2}$ and

$N_m = \frac{N_{2,b}+1}{2}$. For Case 2-1, thus, we have:

$$\begin{aligned}
& E[N_t(t_o)|\text{Case2-1}] \\
&= \sum_{i=0}^{\infty} \sum_{k=0}^i (i+1+k) Pr[N_t(t_o) = i+k | N_{2,b} = 2i+1] \\
&\quad \times Pr[N_{2,b} = 2i+1] \\
&= \sum_{i=0}^{\infty} \sum_{k=0}^i [(i+1+k) \binom{i}{k} \alpha^k (1-\alpha)^{i-k}] Pr[N_{2,b} = 2i+1] \\
&= \sum_{i=1}^{\infty} [1 + (1+\alpha)i] \left(\frac{\eta_f}{\eta_s}\right) [1 - f_f^*(\eta_s)] [1 - f_m^*(\eta_s)] [f_m^*(\eta_s) f_f^*(\eta_s)]^i \\
&= \frac{\eta_f [1 - f_f^*(\eta_s)] [1 - f_m^*(\eta_s)] [1 + \alpha f_m^*(\eta_s) f_f^*(\eta_s)]}{\eta_s (1 - f_m^*(\eta_s) f_f^*(\eta_s))^2}. \tag{11}
\end{aligned}$$

Case 2-2: The number of cell crossings is even, i.e., $N_{2,b} = 2i, \forall i \in \mathbb{N}_{>0}$, and $N_f = N_m = \frac{N_{2,b}}{2}$. For Case 2-2, thus, we have:

$$\begin{aligned}
& E[N_t(t_o)|\text{Case2-2}] \\
&= \sum_{i=1}^{\infty} \left(\beta + \sum_{k=0}^{i-1} (i+k) Pr[N_t(t_o) = i+k | N_{2,b} = 2i] \right) \\
&\quad \times Pr[N_{2,b} = 2i] \\
&= \sum_{i=1}^{\infty} \left(\beta + \sum_{k=0}^{i-1} (i+k) \binom{i-1}{k} \alpha^k (1-\alpha)^{i-1-k} \right) Pr[N_{2,b} = 2i] \\
&= \sum_{i=1}^{\infty} [(i+\alpha)i - \alpha + \beta] \left(\frac{\eta_f}{\eta_s}\right) f_m^*(\eta_s) [1 - f_f^*(\eta_s)]^2 [f_m^*(\eta_s) f_f^*(\eta_s)]^{i-1} \\
&= \frac{\eta_f f_m^*(\eta_s) [1 - f_f^*(\eta_s)]^2 [1 + \beta + (\alpha - \beta) f_m^*(\eta_s) f_f^*(\eta_s)]}{\eta_s (1 - f_m^*(\eta_s) f_f^*(\eta_s))^2}. \tag{12}
\end{aligned}$$

By applying (3), (4), (9), (10), (11), and (12) into (8), we obtain:

$$\begin{aligned}
& E[N_t(t_o)] \\
&= (1+\alpha)X_1 + [1 + \beta + (1 + 2\alpha - \beta) f_m^*(\eta_s) f_f^*(\eta_s)] X_2 \\
&\quad + [1 + \beta + (\alpha - \beta) f_m^*(\eta_s) f_f^*(\eta_s)] X_3, \tag{13}
\end{aligned}$$

where

$$\begin{aligned} X_1 &= \frac{\eta_f \eta_m f_f^*(\eta_s) [1 - f_m^*(\eta_s)]^2}{\eta_s (\eta_f + \eta_m) (1 - f_m^*(\eta_s) f_f^*(\eta_s))^2}, \\ X_2 &= \frac{\eta_f \eta_m [1 - f_f^*(\eta_s)] [1 - f_m^*(\eta_s)]}{\eta_s (\eta_f + \eta_m) (1 - f_m^*(\eta_s) f_f^*(\eta_s))^2}, \\ X_3 &= \frac{\eta_f \eta_m f_f^*(\eta_s) [1 - f_m^*(\eta_s)]^2}{\eta_s (\eta_f + \eta_m) (1 - f_f^*(\eta_s) f_m^*(\eta_s))^2}. \end{aligned}$$

Therefore, our first performance metric $\Theta(t_o)$ can be obtained by:

$$\Theta(t_o) = \frac{E[N_b] - E[N_t(t_o)]}{E[N_b]} = \frac{\eta_s + \eta_o f_f^*(\eta_s + \eta_o)}{2(\eta_s + \eta_o)}. \quad (14)$$

B. Derivation of Offloading Capability Loss Ratio $\Lambda(t_o)$

Recall that $\Lambda(t_o) = E[T_t(t_o)]/E[T_b]$. We first derive $E[T_b]$ for the baseline scheme without TO and then $E[T_t(t_o)]$ for the TO algorithm.

1) *Derivation of $E[T_b]$* : For the baseline scheme, let τ be the average residual life of t_{f_0} during t_s , i.e., the average offloading time in t_{f_0} . We then have:

$$\begin{aligned} \tau &= E[\psi_f | t_s > \psi_f] \\ &= \frac{\int_{t_{\psi_f}=0}^{\infty} \int_{t_s=t_{\psi_f}}^{\infty} t_{\psi_f} f_{\psi_f}(t_{\psi_f}) \eta_s e^{-\eta_s t_s} dt_s dt_{\psi_f}}{Pr[t_s > \psi_f]} \\ &= \frac{E[t_{\psi_f} e^{-\eta_s t_{\psi_f}}]}{f_{\psi_f}^*(\eta_s)}. \end{aligned} \quad (15)$$

Let σ be the average age for t_{f_i} during t_s , where the session ends in this t_{f_i} , i.e., the average offloading time in the last t_{f_i} . According to the residual life theorem [20], we have:

$$\sigma = \tau. \quad (16)$$

Let ξ be the average offloading time in t_{f_i} , where the session does not start or end in this t_{f_i} .

We then have:

$$\begin{aligned}
\xi &= E[t_f | t_s > t_f] \\
&= \frac{\int_{t_f=0}^{\infty} \int_{t_s=t_f}^{\infty} t_f f_f(t_f) \eta_s e^{-\eta_s t_s} dt_s dt_f}{Pr[t_s > t_f]} \\
&= \frac{E[t_f e^{-\eta_s t_f}]}{f_f^*(\eta_s)}. \tag{17}
\end{aligned}$$

Again, $E[T_b]$ can be derived from the four scenarios and be expressed as:

$$E[T_b] = Pr[\text{Case1}]E[T_b|\text{Case1}] + Pr[\text{Case2}]E[T_b|\text{Case2}]. \tag{18}$$

Case 1-1: Given $N_{1,b} = 2i, \forall i \in \mathbb{N}_{>0}, N_f = N_m = i$, the total offloading time during t_s is $\sum_{j=1}^i t_{f_j}$. Thus, we have:

$$\begin{aligned}
&E[T_b|\text{Case1-1}] \\
&= \sum_{i=1}^{\infty} E[(\sum_{j=1}^i t_{f_j}) | N_{1,b} = 2i] Pr[N_{1,b} = 2i] \\
&= \sum_{i=1}^{\infty} i \xi \left(\frac{\eta_m}{\eta_s}\right) f_f^*(\eta_s) [1 - f_m^*(\eta_s)]^2 [f_m^*(\eta_s) f_f^*(\eta_s)]^{i-1} \\
&= \frac{\eta_m f_f^*(\eta_s) [1 - f_m^*(\eta_s)]^2 \xi}{\eta_s (1 - f_m^*(\eta_s) f_f^*(\eta_s))^2}. \tag{19}
\end{aligned}$$

Case 1-2: Given $N_{1,b} = 2i + 1, \forall i \in \mathbb{N}, N_f = i + 1$ and $N_m = i$, the total offloading time during t_s is $(\sum_{j=1}^i t_{f_j}) + t_{s_{i+1}}$. Thus, we have:

$$\begin{aligned}
&E[T_b|\text{Case1-2}] \\
&= \sum_{i=0}^{\infty} E[(\sum_{j=1}^i t_{f_j}) + t_{s_{i+1}} | N_{1,b} = 2i + 1] Pr[N_{1,b} = 2i + 1] \\
&= \sum_{i=1}^{\infty} (i\xi + \sigma) \left(\frac{\eta_m}{\eta_s}\right) [1 - f_f^*(\eta_s)] [1 - f_m^*(\eta_s)] [f_m^*(\eta_s) f_f^*(\eta_s)]^i \\
&= \frac{\eta_m [1 - f_f^*(\eta_s)] [1 - f_m^*(\eta_s)] [\sigma + (\xi - \sigma) f_m^*(\eta_s) f_f^*(\eta_s)]}{\eta_s (1 - f_m^*(\eta_s) f_f^*(\eta_s))^2}. \tag{20}
\end{aligned}$$

Case 2-1: Given $N_{2,b} = 2i + 1, \forall i \in \mathbb{N}, N_f = i$ and $N_m = i + 1$, the total offloading time

during t_s is $\psi_f + \sum_{j=1}^i t_{f_j}$. Thus, we have:

$$\begin{aligned}
& E[T_b | \text{Case2-1}] Pr[\text{Case2-1}] \\
&= \sum_{i=0}^{\infty} E[\psi_f + \sum_{j=1}^i t_{f_j} | N_{2,b} = 2i + 1] Pr[N_{2,b} = 2i + 1] \\
&= \sum_{i=1}^{\infty} (\tau + i\xi) \left(\frac{\eta_f}{\eta_s}\right) [1 - f_f^*(\eta_s)] [1 - f_m^*(\eta_s)] [f_m^*(\eta_s) f_f^*(\eta_s)]^i \\
&= \frac{\eta_f [1 - f_f^*(\eta_s)] [1 - f_m^*(\eta_s)] [\tau + (\xi - \tau) f_m^*(\eta_s) f_f^*(\eta_s)]}{\eta_s (1 - f_m^*(\eta_s) f_f^*(\eta_s))^2}. \tag{21}
\end{aligned}$$

Case 2-2: Given $N_b = 2i$, $\forall i \in \mathbb{N}_{>0}$, $N_f = N_m = i$, the total offloading time during t_s is $\psi_f + (\sum_{j=1}^{i-1} t_{f_j}) + t_{s_i}$. Thus, we have:

$$\begin{aligned}
& E[T_b | \text{Case2-2}] Pr[\text{Case2-2}] \\
&= \sum_{i=1}^{\infty} E[\psi_f + (\sum_{j=1}^{i-1} t_{f_j}) + t_{s_i} | N_{2,b} = 2i] Pr[N_{2,b} = 2i] \\
&= \sum_{i=1}^{\infty} [\tau + (i-1)\xi + \sigma] \left(\frac{\eta_f}{\eta_s}\right) f_m^*(\eta_s) [1 - f_f^*(\eta_s)]^2 \\
&\quad \times [f_m^*(\eta_s) f_f^*(\eta_s)]^{i-1} \\
&= \frac{\eta_f f_f^*(\eta_s) [1 - f_m^*(\eta_s)]^2 [\tau + \sigma + (\xi - \tau - \sigma) f_m^*(\eta_s) f_f^*(\eta_s)]}{\eta_s \eta_f (1 - f_m^*(\eta_s) f_f^*(\eta_s))^2}. \tag{22}
\end{aligned}$$

By applying (3), (4), (19), (20), (21), and (22) into (18), we obtain:

$$\begin{aligned}
& E[T_b] \\
&= \xi X_1 + [\tau + \sigma + (2\xi - \tau - \sigma) f_m^*(\eta_s) f_f^*(\eta_s)] X_2 \\
&\quad + [\tau + \sigma + (\xi - \tau - \sigma) f_m^*(\eta_s) f_f^*(\eta_s)] X_3, \tag{23}
\end{aligned}$$

where X_1 , X_2 , and X_3 are the same as those in Eq. (13).

2) *Derivation of $E[T_t(t_o)]$* : For the TO algorithm, let ϕ be the average offloading time for t_{f_i} during t_s , where the session does not start or end in this t_{f_i} . We then have:

$$\begin{aligned}
\phi &= E[t_{f_i} - t_o | (t_o < t_{f_i} | t_{f_i} < t_{s_i})] \\
&= \int_{t_o=0}^{\infty} \int_{t_{f_i}=t_o}^{\infty} \int_{t_{s_i}=t_{f_i}}^{\infty} (t_{f_i} - t_o) \\
&\quad \times \frac{\eta_o e^{-\eta_o t_o} f_f(t_{f_i}) \eta_s e^{-\eta_s t_{s_i}}}{Pr[t_o < t_{f_i} | t_{f_i} < t_{s_i}] Pr[t_{f_i} < t_{s_i}]} dt_{s_i} dt_{f_i} dt_o \\
&= \frac{E[t_{f_i} e^{-\eta_s t_{f_i}}] + \frac{1}{\eta_o} (f_f^*(\eta_s + \eta_o) - f_f^*(\eta_s))}{\alpha f_f^*(\eta_s)}. \tag{24}
\end{aligned}$$

Let ρ be the average offloading time for t_{f_i} during t_s , where the session ends in this t_{f_i} . We then have:

$$\begin{aligned}
\rho &= E[t_{s_i} - t_o | (t_o < t_{s_i} | t_{s_i} < t_{f_i})] \\
&= \int_{t_o=0}^{\infty} \int_{t_{s_i}=t_o}^{\infty} \int_{t_{f_i}=t_{s_i}}^{\infty} (t_{s_i} - t_o) \\
&\quad \times \frac{\eta_o e^{-\eta_o t_o} \eta_s e^{-\eta_s t_{s_i}} f_f(t_{f_i})}{Pr[t_o < t_{s_i} | t_{s_i} < t_{f_i}] Pr[t_{s_i} < t_{f_i}]} dt_{f_i} dt_{s_i} dt_o \\
&= \frac{\frac{1}{\eta_s} + (\frac{1}{\eta_o} - \frac{1}{\eta_s}) f_f^*(\eta_s) - E[t_{f_i} e^{-\eta_s t_{f_i}}] - \frac{\eta_o + \eta_s f_f^*(\eta_s + \eta_o)}{\eta_o(\eta_s + \eta_o)}}{\beta(1 - f_f^*(\eta_s))}. \tag{25}
\end{aligned}$$

Similar to the derivation of $E[T_b]$, we express $E[T_t(t_o)]$ as:

$$\begin{aligned}
&E[T_t(t_o)] \\
&= Pr[\text{Case1}] E[T_t(t_o) | \text{Case1}] + Pr[\text{Case2}] E[T_t(t_o) | \text{Case2}]. \tag{26}
\end{aligned}$$

Let N_h be the total number of macrocell-to-femtocell handovers during t_s . $E[T_t(t_o)]$ is derived from the four scenarios as follows:

Case 1-1: Given $N_{1,b} = 2i$, $N_f = i$, $\forall i \in \mathbb{N}_{>0}$, N_h is in the range $0 \leq N_h \leq i$. The average

offloading time during t_s is $(\sum_{j=0}^i j\phi Pr[N_h = j])$. Thus, we have:

$$\begin{aligned}
& E[T_t(t_o)|\text{Case1-1}] \\
&= \sum_{i=1}^{\infty} \sum_{k=0}^i (k\phi) Pr[N_h = k|N_{1,b} = 2i] Pr[N_{1,b} = 2i] \\
&= \sum_{i=1}^{\infty} \sum_{k=0}^i [(k\phi) \binom{i}{k} \alpha^k (1-\alpha)^{i-k}] Pr[N_{1,b} = 2i] \\
&= \sum_{i=1}^{\infty} [\alpha\phi i] \left(\frac{\eta_m}{\eta_s}\right) f_f^*(\eta_s) [1 - f_m^*(\eta_s)]^2 [f_m^*(\eta_s) f_f^*(\eta_s)]^{i-1} \\
&= \frac{\eta_m f_f^*(\eta_s) [1 - f_m^*(\eta_s)]^2 (\alpha\phi)}{\eta_s (1 - f_m^*(\eta_s) f_f^*(\eta_s))^2}. \tag{27}
\end{aligned}$$

Case 1-2: Given $N_{1,b} = 2i + 1$, $N_f = i + 1$, $\forall i \in \mathbb{N}$, N_h is in the range $1 \leq N_h \leq i + 1$. The average offloading time during t_s is $(\beta\rho + \sum_{j=0}^i j\phi Pr[N_h = j + 1])$. Thus, we have:

$$\begin{aligned}
& E[T_t(t_o)|\text{Case1-2}] \\
&= \sum_{i=0}^{\infty} \left(\beta\rho + \sum_{k=0}^i (k\phi) Pr[N_h = k + 1|N_{1,b} = 2i + 1] \right) \\
&\quad \times Pr[N_{1,b} = 2i + 1] \\
&= \sum_{i=0}^{\infty} \left(\beta\rho + \sum_{k=0}^i (k\phi) \binom{i}{k} \alpha^k (1-\alpha)^{i-k} \right) \\
&\quad \times Pr[N_{1,b} = 2i + 1] \\
&= \sum_{i=0}^{\infty} [\alpha\phi i + \beta\rho] \left(\frac{\eta_m}{\eta_s}\right) [1 - f_f^*(\eta_s)] [1 - f_m^*(\eta_s)] \\
&\quad \times [f_m^*(\eta_s) f_f^*(\eta_s)]^i \\
&= \frac{\eta_m [1 - f_f^*(\eta_s)] [1 - f_m^*(\eta_s)] [\beta\rho + (\alpha\phi - \beta\rho) f_m^*(\eta_s) f_f^*(\eta_s)]}{\eta_s (1 - f_m^*(\eta_s) f_f^*(\eta_s))^2}. \tag{28}
\end{aligned}$$

Case 2-1: Given $N_{2,b} = 2i + 1$, $N_f = i$, $\forall i \in \mathbb{N}$, N_h is in the range $0 \leq N_h \leq i$. The average

offloading time during t_s is $(\tau + \sum_{j=0}^i j\phi Pr[N_h = j])$. Thus, we have:

$$\begin{aligned}
& E[T_t(t_o)|\text{Case2-1}] \\
&= \sum_{i=0}^{\infty} \left(\tau + \sum_{k=0}^i (k\phi) Pr[N_h = k | N_{2,b} = 2i + 1] \right) \\
&\quad \times Pr[N_{2,b} = 2i + 1] \\
&= \sum_{i=0}^{\infty} \left(\tau + \sum_{k=0}^i (k\phi) \binom{i}{k} \alpha^k (1 - \alpha)^{i-k} \right) \\
&\quad \times Pr[N_{2,b} = 2i + 1] \\
&= \sum_{i=0}^{\infty} [\tau + \alpha\phi i] \left(\frac{\eta_f}{\eta_s} \right) [1 - f_f^*(\eta_s)] [1 - f_m^*(\eta_s)] [f_m^*(\eta_s) f_f^*(\eta_s)]^i \\
&= \frac{\eta_f [1 - f_f^*(\eta_s)] [1 - f_m^*(\eta_s)] [\tau + (\alpha\phi - \tau) f_m^*(\eta_s) f_f^*(\eta_s)]}{\eta_s (1 - f_m^*(\eta_s) f_f^*(\eta_s))^2}. \tag{29}
\end{aligned}$$

Case 2-2: Given $N_{2,b} = 2i$, $N_f = i$, $\forall i \in \mathbb{N}_{>0}$, N_h is in the range $1 \leq N_h \leq i$. The average offloading time during t_s is $(\tau + \beta\rho + \sum_{j=0}^{i-1} j\phi Pr[N_h = j + 1])$. Thus, we have:

$$\begin{aligned}
& E[T_t(t_o)|\text{Case2-2}] \\
&= \sum_{i=1}^{\infty} \left(\tau + \beta\rho + \sum_{k=0}^{i-1} (k\phi) Pr[N_h = k + 1 | N_{2,b} = 2i] \right) Pr[N_{2,b} = 2i] \\
&= \sum_{i=1}^{\infty} \left(\tau + \beta\rho + \sum_{k=0}^{i-1} (k\phi) \binom{i-1}{k} \alpha^k (1 - \alpha)^{i-1-k} \right) Pr[N_{2,b} = 2i] \\
&= \sum_{i=1}^{\infty} [\tau + \beta\rho + \alpha\phi(i-1)] \left(\frac{\eta_f}{\eta_s} \right) f_m^*(\eta_s) [1 - f_f^*(\eta_s)]^2 [f_m^*(\eta_s) f_f^*(\eta_s)]^{i-1} \\
&= \frac{\eta_m f_m^*(\eta_s) [1 - f_f^*(\eta_s)]^2 [\tau + \beta\rho]}{\eta_s (1 - f_m^*(\eta_s) f_f^*(\eta_s))^2} \\
&\quad + \frac{\eta_m f_m^*(\eta_s) [1 - f_f^*(\eta_s)]^2 [(\alpha\phi - \tau - \beta\rho) f_m^*(\eta_s) f_f^*(\eta_s)]}{\eta_s (1 - f_m^*(\eta_s) f_f^*(\eta_s))^2}. \tag{30}
\end{aligned}$$

By applying (3), (4), (27), (28), (29), and (30) into (26), we have:

$$\begin{aligned}
& E[T_i(t_o)] \\
& = \alpha\phi X_1 + [\tau + \beta\rho + (2\alpha\phi - \tau - \beta\rho)f_m^*(\eta_s)f_f^*(\eta_s)]X_2 \\
& \quad + [\tau + \beta\rho + (\alpha\phi - \tau - \beta\rho)f_m^*(\eta_s)f_f^*(\eta_s)]X_3,
\end{aligned} \tag{31}$$

where X_1 , X_2 , and X_3 are the same as those in Eq. (13).

Therefore, our second performance metric $\Lambda(t_o)$ can be obtained by:

$$\Lambda(t_o) = \frac{E[T_i(t_o)]}{E[T_b]} = \frac{\eta_f\eta_o - \eta_f(\eta_s + \eta_o)f_f^*(\eta_s) + \eta_f\eta_s f_f^*(\eta_s + \eta_o) + \eta_s^2(\eta_s + \eta_o)Y_2}{\eta_s(\eta_s + \eta_o)(\eta_f Y_1 + 2\eta_s Y_2)}. \tag{32}$$

where $Y_1 = E[t_f e^{-\eta_s t_f}]$ and $Y_2 = E[t_{\psi_f} e^{-\eta_s t_{\psi_f}}]$.

VI. SIMULATION AND NUMERICAL RESULTS

In this section, we provide numerical results for the analysis presented in Section V. The analysis is validated through extensive simulations by using ns-2 [22], version 2.35. In addition, the errors between the analytical and simulated results are verified to fall within one percent. Due to page limitation, we only show one table of our results, Table II.

The two performance metrics, i.e., (14) and (32), can be organized into a meaningful form only if $f_f^*(s)$ and $f_m^*(s)$ have closed-form solutions. Thus, we choose to apply Gamma distribution for both femtocell residence time and macrocell residence time because the Gamma distribution has two characteristics: (1) it is a more general kind of distribution and can approximate many other distributions, and (2) a closed-form Laplace transform solution for it exists. Also, the Gamma distribution has been commonly adopted in many previous papers (e.g. [19], [23]) to study various UE mobility behaviors.

Then, we observe that two factors affects the performance of our proposed TO: the effects of UE mobility and the session length. Their impact are investigated and the results are illustrated in Figs. 5–7.

A. Effects of UE Mobility

As shown in Eqs. (14) and (32), the UE's behavior inside the macrocell (η_m and v_m) have no impacts on the two performance metrics, the effects of UE mobility can be simply reflected by

TABLE II: Validation of analytical and simulated results.

$\eta_m = 10\eta_s, v_m = 1/\eta_m, \eta_f = 10\eta_s, v_f = 1000/\eta_f$					
$1/\eta_o$ (unit: $1/\eta_s$)		0.1	0.2	0.3	0.4
$N_t(t_o)$	Analytical	5.74007	5.55835	5.45672	5.38896
	Simulated	5.75666	5.53744	5.45196	5.38116
	Error (%)	0.28899	0.37618	0.08718	0.14468
$T_t(t_o)$	Analytical	192.43505	169.83760	154.62965	143.48846
	Simulated	191.97960	168.85753	155.70437	142.10245
	Error (%)	0.23688	0.57707	0.69503	0.96593
$\Theta(t_o)$	Analytical	42.59933	44.41655	45.43281	46.11039
	Simulated	42.59930	44.42310	45.40490	46.12440
	Error (%)	0.00008	0.01476	0.06143	0.03038
$\Lambda(t_o)$	Analytical	81.25140	71.71013	65.28891	60.58480
	Simulated	81.14890	71.63550	65.33060	60.46900
	Error (%)	0.12615	0.10408	0.06385	0.19113

the UE's behavior inside femtocells, i.e., η_f and v_f .

First, the effects of mean femtocell residence time (FRT), $1/\eta_f$, are investigated. In Fig. 5, the mean macrocell residence time (MRT), $1/\eta_m$, is fixed as one tenth of the session length ($\eta_m = 10\eta_s$), and the mean FRT is set from one hundredth of the session length ($\eta_f = 100\eta_s$) to ten times of that ($\eta_f = 0.1\eta_s$). Generally, for the cases that the mean FRT take smaller portion of the session length, the proposed TO has better performance in terms of $\Theta(t_o)$. For example, in the green-diamond line, the proposed TO can easily reduce over 40% signaling overhead but lose less than 10% femtocell offloading capability. In addition, $\Theta(t_o)$ increases faster than $\Lambda(t_o)$ drops as $E[t_o]$ rises. Thus, the proposed TO is proven to be capable of significantly reducing signaling overhead at a minor cost of femtocell offloading capability.

Second, the effects of the variance of FRT, v_f , are investigated. A larger variance indicates that the UE mobility behavior is more dynamic and less predictable, which fits closer to real life situation. In Fig. 6, the mean MRT and the mean FRT are fixed as one tenth of the session length ($\eta_m = 10\eta_s$) and one fortieth of the session length ($\eta_f = 40\eta_s$), respectively. The variance v_f is set from one hundredth of mean FRT ($v_f = 1/100\eta_f$) to a thousand times of mean FRT ($v_f = 1000/\eta_f$). As shown in Fig. 6, both $\Theta(t_o)$ and $\Lambda(t_o)$ have better performance when the variance v_f gets larger for all different mean values of the offloading threshold. Therefore, the

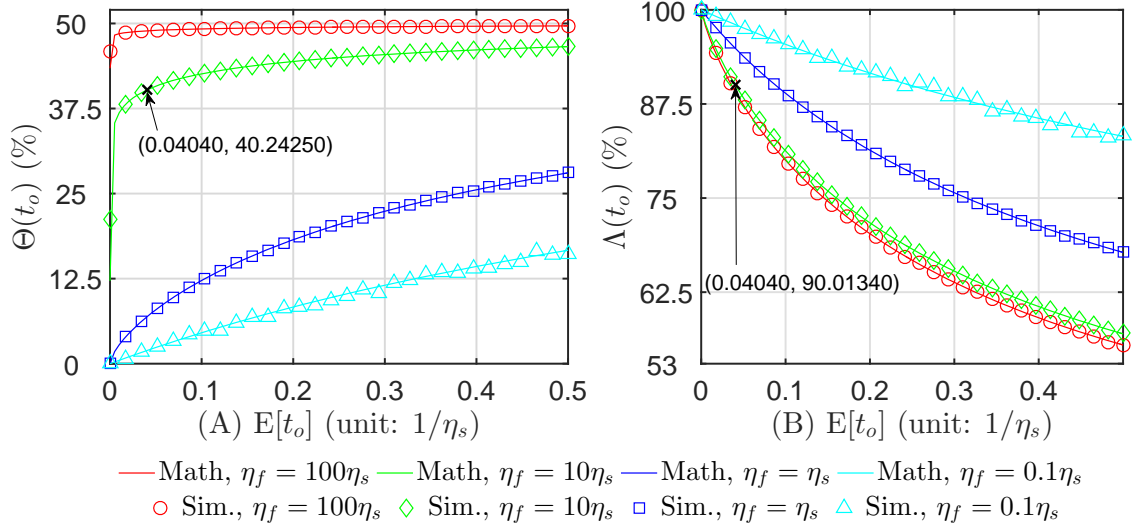


Fig. 5: The effects of mean femtocell residence time η_f on $\Theta(t_o)$ and $\Lambda(t_o)$ ($\eta_m = 10\eta_s$).

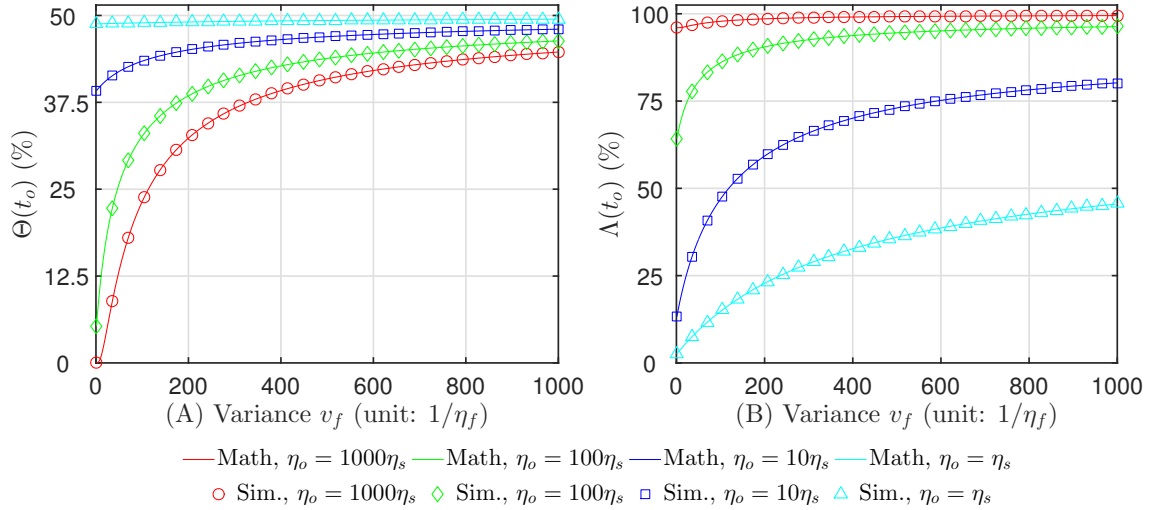


Fig. 6: The effects of variance of femtocell residence time v_f on $\Theta(t_o)$ and $\Lambda(t_o)$ ($\eta_m = 10\eta_s$, $\eta_f = 40\eta_s$).

proposed TO is considered effective against various UE mobility behaviors in real life.

B. Effects of Session Length

In Fig. 7, the mean MRT and the mean FRT are fixed as 60 and 15 seconds, respectively. The mean session length is set from 0 to 150 seconds (i.e., $10/\eta_f$). We observe that the mean session length has prominent effects on the two performance metrics only when it is smaller than the mean FRT, i.e., $\eta_s > \eta_f$, while it tends to be less perceivable when $\eta_s < \eta_f$. In the case of

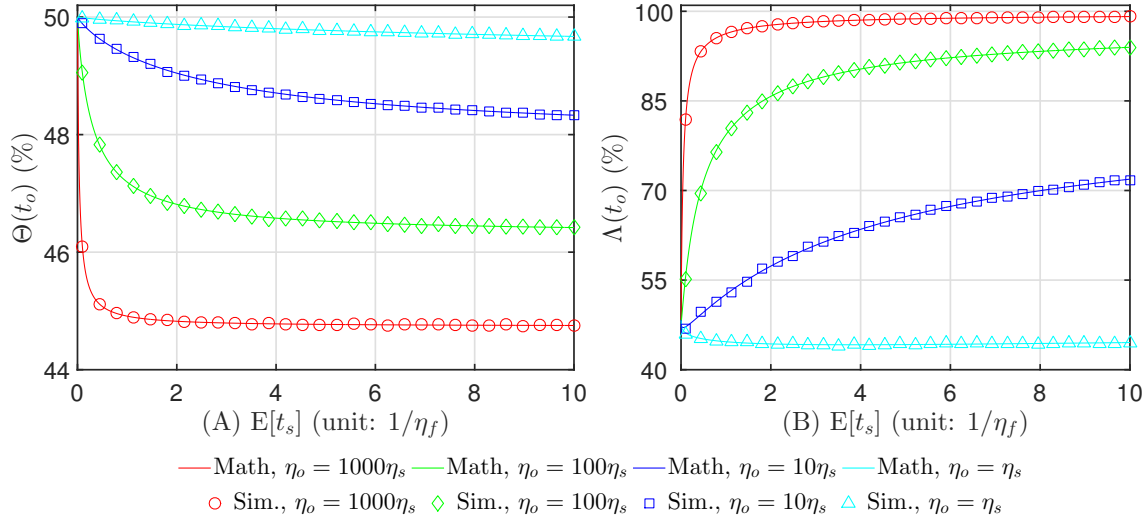


Fig. 7: The effects of mean session length η_s on $\Theta(t_o)$ and $\Lambda(t_o)$ ($1/\eta_m = 60s$, $1/\eta_f = 15s$).

$\eta_s > \eta_f$, $\Theta(t_o)$ decreases when the session length increases. It is because the offloading threshold takes smaller proportion of the session length when t_s gets larger. On the other hand, for $\eta_s > \eta_f$, $\Lambda(t_o)$ increases when the session length increases because the offloading time lengthens along with the session length. Thus, depending on whether the mean session length is smaller than the mean FRT, the significance of the session length can be determined. Overall, for $\eta_s > \eta_f$, both UE mobility behaviors and the session length have impacts on the two performance metrics, while the effects of UE mobility dominate for the case of $\eta_s < \eta_f$.

VII. OPTIMAL TO ALGORITHM

A. Determination of Optimal Offloading Threshold

It is of high priority for network operators to select a proper offloading threshold t_o , such that the TO algorithm is efficient. A large offloading threshold t_o will reduce massive network signaling overhead but sacrifice femtocell offloading capability. On the other hand, a small offloading threshold t_o reserves more femtocell offloading capability but costs higher network signaling overhead. Recall that t_o is an exponential random variable, and our goal is to find the optimal mean offloading threshold, aka the optimal distribution, such that $\Theta(t_o)$ and $\Lambda(t_o)$ together achieve maximum. From Eqs. (14) and (32), both $\Theta(t_o)$ and $\Lambda(t_o)$ are functions of η_o , thus we formulate the objective function as:

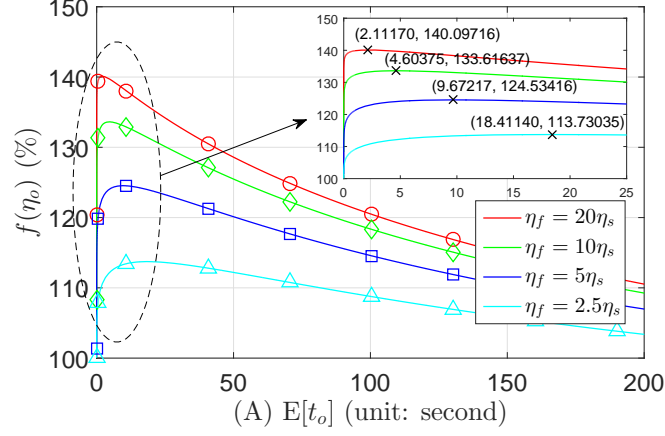


Fig. 8: Determination of the optimal offloading threshold.

$$\begin{aligned} & \underset{\eta_o}{\text{maximize}} && f(\eta_o) = \Theta(\eta_o) + \Lambda(\eta_o) \\ & \text{subject to} && 0 < \eta_o \leq \delta, \end{aligned} \quad (33)$$

where δ is the upperbound of η_o , which can be determined by operators according to their historical statistic data, and define the optimal offloading threshold as:

$$E[t_o]^* = \frac{1}{\eta_o^*}. \quad (34)$$

Then, according to Calculus, such η_o^* can be found by solving the differential equation $f'(\eta_o) = 0$ and checking the boundary values, i.e., $f(0)$ and $f(\delta)$. Since the closed-form solution to the differential equation does not have a meaningful and simplified expression, we instead acquire the answer by using MATLAB. The mean computing time for the η_o^* obtained by using a normal PC (Intel Core i5-3470 with 8G RAM) is 121.56 ms with the standard deviation of 1.97 ms.

Fig. 8 illustrates a graphical plot of $f(\eta_o)$ with 4 different settings. In this example, the session length t_s and the upperbound δ are set as 600 second and 200 second, respectively. We solve the equation $f'(\eta_o) = 0$ and compare it with the boundary values for each line, and the maximum values are denoted as crosses in the figure. For the green line ($\eta_f = 10\eta_s$), the optimal offloading threshold $E[t_o]^*$ is computed as 4.60375, with the corresponding η_o^* as 0.21721. Thus, operators can achieve the best performance for the TO algorithm by setting the optimal η_o^* .

Algorithm 1 Selecting an optimal offloading threshold.

Input: δ **Output:** η_o^* **Ensure:** $\eta_o^* \in (0, \delta]$

```

1: if  $f'(\eta_o) = 0$  has a real solution  $\eta'_o$  then
2:   if  $f(\delta) > f(0)$  then
3:     if  $f(\eta'_o) > f(\delta)$  then
4:       return  $\eta'_o$ 
5:     else
6:       return  $f(\delta)$ 
7:     end if
8:   else
9:     if  $f(\eta'_o) > f(0)$  then
10:      return  $\eta'_o$ 
11:    else
12:      return  $f(0)$ 
13:    end if
14:   end if
15: else if  $f(\delta) > f(0)$  then
16:   return  $\delta$ 
17: else
18:   return 0
19: end if

```

Next, we propose an algorithm (shown as Algorithm 1) to systematically find η_o^* . Algorithm 1 takes one input value: δ , which is the upperbound for η_o . Again, operators can refer to their historical statistics on femtocell CRT and determine δ accordingly. First, Algorithm 1 checks if $f'(\eta_o) = 0$ has a real solution, say, η'_o . If no, then return the larger boundary value. Otherwise, it compares η'_o with the two boundary values, and return whichever the largest as the optimal offloading threshold. Note that when η_o^* is returned as 0, $E[t_o]^*$ would go to infinity. In practice, this can be solved by just setting η_o^* as an arbitrary small number.

B. Implementation Issues

To use the TO algorithm, we need to gather statistics of $E[t_f]$, $E[t_m]$, and $E[t_s]$ in advance. First, HeNBs can continuously collect each UE's duration in the femtocells by observing the time stamps when it performs handover in and handover out. The HeNBs then upload their own $E[t_f]$ to the eNB, which in turn will compute a combined $E[t_f]$ from all HeNBs. Note that the frequency for uploading $E[t_f]$ involves the tradeoff between the precision of the TO algorithm

and extra signaling overhead. Second, eNBs can obtain $E[t_m]$ when HeNBs obtain $E[t_f]$. Last, $E[t_s]$ can be acquired by recording the lifetime of traffic flows at the entities in the core network, such as P-GW or Policy Charging Rule Function (PCRF) [24].

VIII. CONCLUSIONS

In this paper, we propose the TO algorithm by considering the trade-off between network signaling overhead and femtocell offloading capability. The TO algorithm is evaluated by two performance metrics: signaling overhead reduction ratio $\Theta(t_o)$ and offloading capability loss ratio $\Lambda(t_o)$. Our analytical model and simulation results show consistent findings that the proposed TO algorithm is capable of significantly reducing signaling overhead against various UE mobility behaviors while little femtocell offloading capability is compromised, particularly for UEs with more dynamic mobility behaviors (i.e., larger v_f). Moreover, our work provides guidelines for network operators on how to set an optimal offloading threshold to achieve the best performance.

REFERENCES

- [1] 3GPP TS 36.300 V12.5.0, *Evolved Universal Terrestrial Radio Access (E-UTRA) and Evolved Universal Terrestrial Radio Access Network (E-UTRAN); Overall description; Stage 2 (Release 12)*, Std., Mar. 2015.
- [2] “2014 Annual Report,” AT&T, Tech. Rep., 2014.
- [3] “Cisco Visual Networking Index: Global Mobile Data Traffic Forecast Update 2014V2019 White Paper,” Cisco, Tech. Rep., Feb. 2015.
- [4] “Small Cell Forum,” <http://www.smallcellforum.org/>.
- [5] V. Chandrasekhar, J. G. Andrews, and A. Gatherer, “Femtocell networks: a survey,” *IEEE Commun. Mag.*, vol. 46, no. 9, pp. 59–67, 2008.
- [6] “Urban small cells in the real world: case studies,” Small Cell Forum, Tech. Rep., 2014.
- [7] M. Z. Chowdhury, W. Ryu, E. Rhee, and Y. M. Jang, “Handover between macrocell and femtocell for UMTS based networks,” in *Proc. IEEE 11th Int’l Conf. Advanced Communication Technology, ICACT*, 2009, pp. 237–241.
- [8] J.-S. Kim and T.-J. Lee, “Handover in UMTS networks with hybrid access femtocells,” in *Proc. IEEE 12th Int’l Conf. Advanced Communication Technology, ICACT*, vol. 1, 2010, pp. 904–908.
- [9] C.-P. Lee, K.-F. Huang, P. Lin, H.-J. Su, and C.-L. Wang, “Reducing handover cost for LTE femtocell/macrocell network,” in *Proc. IEEE GLOBECOM*, 2013, pp. 4988–4993.
- [10] W. Shaohong, Z. Xin, Z. Ruiming, Y. Zhiwei, F. Yinglong, and Y. Dacheng, “Handover study concerning mobility in the two-hierarchy network,” in *Proc. IEEE Veh. Technol. Conf., VTC*, 2009, pp. 1–5.
- [11] A. Ulvan, R. Bestak, and M. Ulvan, “The study of handover procedure in LTE-based femtocell network,” in *Proc. 3rd Joint IFIP Wireless and Mobile Networking Conference, WMNC*, 2010, pp. 1–6.

- [12] H. Zhang, X. Wen, B. Wang, W. Zheng, and Y. Sun, "A novel handover mechanism between femtocell and macrocell for LTE based networks," in *Proc. IEEE Int'l Conf. Communication Software and Networks, ICCSN*, 2010, pp. 228–231.
- [13] G. Yang, X. Wang, and X. Chen, "Handover control for LTE femtocell networks," in *Proc. IEEE Int'l Conf. Electronics, Communications and Control, ICECC*, 2011, pp. 2670–2673.
- [14] W.-H. Chen, Y. Ren, and J.-C. Chen, "Design and analysis of a threshold offloading (TO) algorithm for LTE femtocell/macrocell networks," in *2016 IEEE Symposium on Computers and Communication (ISCC)*, to be published.
- [15] 3GPP TS 36.331 V12.5.0, *LTE; Evolved Universal Terrestrial Radio Access (E-UTRA); Radio Resource Control (RRC); Protocol specification (Release 12)*, Std., Apr. 2015.
- [16] A. Balasubramanian, R. Mahajan, and A. Venkataramani, "Augmenting mobile 3G using WiFi," in *Proc. ACM 8th int'l Conf. Mobile systems, applications, and services*, 2010, pp. 209–222.
- [17] T. Han and N. Ansari, "Enabling mobile traffic offloading via energy spectrum trading," *IEEE Trans. Wireless Commun.*, vol. 13, no. 6, pp. 3317–3328, Jun. 2014.
- [18] K. Lee, J. Lee, Y. Yi, I. Rhee, and S. Chong, "Mobile data offloading: How much can WiFi deliver?" *IEEE/ACM Trans. Netw.*, vol. 21, no. 2, pp. 536–550, 2013.
- [19] R.-H. Liou, Y.-B. Lin, and S.-C. Tsai, "An investigation on LTE mobility management," *IEEE Trans. Mobile Comput.*, vol. 12, no. 1, pp. 166–176, 2013.
- [20] S. M. Ross, *Introduction to probability models*. Academic press, 2014.
- [21] H.-L. Fu, P. Lin, and Y.-B. Lin, "Reducing signaling overhead for femtocell/macrocell networks," *IEEE Trans. Mobile Comput.*, vol. 12, no. 8, pp. 1587–1597, 2013.
- [22] "The network simulator - ns-2," <http://www.isi.edu/nsnam/ns/>.
- [23] W. Ma and Y. Fang, "Dynamic hierarchical mobility management strategy for mobile IP networks," *IEEE J. Sel. Areas Commun.*, vol. 22, no. 4, pp. 664–676, 2004.
- [24] 3GPP TS 23.261 V12.0.0, *IP flow mobility and seamless Wireless Local Area Network (WLAN) offload; Stage 2 (Release 12)*, Std., Sep. 2014.